A fully automated unsaturated triaxial device for testing of soils under complicated hydromechanical stress paths

Seyed Mohsen Haeri[1#], *Saman* Soleymani Borujerdi[2], and *Amir* Akbari Garakani[3]

[1]*Professor, Civil Engineering Department, Sharif University of Technology, Tehran, Iran*
[2]*Ph.D. Candidate, Civil Engineering Department, Sharif University of Technology, Tehran, Iran*
[3]*Assistant Professor, Power Industry Structures Research Department, Niroo Research Institute, Tehran, Iran*
[#]*Corresponding author: smhaeri@sharif.edu*

ABSTRACT

A fully-automated unsaturated triaxial device is developed at the Advanced Soil Mechanic Laboratory of the Sharif University of Technology (SUT) to investigate the hydromechanical behavior of unsaturated soils under any complicated path. The main improvements of the developed device are (1) the ability to continuously measure accurately different stress/strain variables during long duration of unsaturated tests. This is of great importance in capturing the sudden deformations of the specimen, under wetting (2) providing a user-friendly controller software enabling the definition of any desired stress/strain variable and stress/strain paths under either stress-controlled or strain-controlled conditions. Finally, to evaluate the performance of the developed apparatus, two wetting tests were carried out to study the effect of initial shear stress on the hydromechanical behavior of unsaturated reconstituted specimens of Gorgan loess. In these wetting tests, the specimens were wetted under isotropic and anisotropic stress states by stepwise reduction of suction to approach to the saturated condition. The obtained results showed the excellent performance of the developed device to accurately follow the defined stress path along with the continuous measurement of stress/strain variables. The tested collapsible soil specimen that was wetted under the effect of initial shear stress exhibited a larger volume decrease accompanied by a larger degree of saturation compared to those of the specimen wetted under the isotropic stress state with the same initial mean net stress.

Keywords: fully automated device; unsaturated triaxial; collapsible soil; initial shear stress.

1. Introduction

A comprehensive experimental study of the hydromechanical behavior of unsaturated soils under different isotropic and anisotropic stress/strain paths requires accurate control and measurement of stress/strain variables during the long duration of unsaturated experiments. This is of great importance, especially in the case of collapsible loessial soils, where it is necessary to continuously measure the stress/strain variables in order to capture the sudden deformations (i.e., collapses) of the specimens (Haeri et al. 2012, 2014, 2017; Garakani et al. 2015; Haeri 2016; Li et al. 2016). Therefore, it is essential to develop a fully-automated unsaturated device with a capability to capture the complete hydromechanical stress/strain path.

There are many cases where anisotropic stress state is present in the nature especially when the soil is near or under a structure or is located on a slope. Therefore, the study of hydromechanical behavior of loessial soils under anisotropic stress states is vital.

In recent years, with the rapid growth of unsaturated soil mechanics and understanding the importance of unsaturated state variables, such as suction and degree of saturation, in governing the hydromechanical behavior of unsaturated soils, an extensive research attempt has been devoted for promotion of the conventional oedometer and triaxial devices to conduct suction-monitored or suction-controlled tests (Kato and Kawai 2000; Pereira and Fredlund 2000; Sun et al. 2004; Jotisankasa et al. 2007; Haeri et al. 2014, 2017; Garakani et al. 2015; Hossen 2015; Zhang et al. 2020). However, only few studies have been focused on the investigation of the hydromechanical behavior of unsaturated and collapsible soils under anisotropic stress paths (Casini et al. 2013; Zhan et al. 2014; Zhou et al. 2014; Borujerdi 2015; Al-Sharrad et al. 2017; Liang et al. 2018; Wang et al. 2019b).

Zhan (2003) performed an experimental program to investigate the wetting-induced softening behavior of an unsaturated expansive soil which was involved in rain-induced slope failures. As part of the study, wetting tests were conducted under anisotropic stress states on unsaturated recompacted and intact specimens. The experimental program was conducted using a fully automated triaxial device. However, the temperature was not controlled as the device was placed in a laboratory with no temperature control. The results showed that for both recompacted and intact specimens, there was a threshold suction value (i.e., yield suction), below which the axial strain increased significantly.

Zhou (2012) studied the failure mechanism of a loess slope subjected to water infiltration through experimental research, a part of which included the wetting tests at constant axial load on unsaturated intact specimens of silty loess using an unsaturated triaxial device. The device was not fully automated, however, it was placed in a temperature-controlled laboratory. The obtained

results revealed that the soil water retention curve (SWRC) of the intact loess was stress-dependent.

Al-Sharrad (2013) conducted an experimental research to investigate the effect of evolving anisotropy on the stress-strain behavior of an unsaturated expansive soil. A part of the study involved suction-controlled anisotropic compression tests on both isotropically and anisotropically compacted specimens using a fully automated triaxial device. The device was placed in a temperature-controlled laboratory that was not heat-insulated. They found that the initial fabric of both isotropically and anisotropically compacted specimens can be altered by plastic straining during either suction equalization or anisotropic compression stages.

Wang et al. (2019b) investigated the mechanism of the wetting-induced failure of an unsaturated loess landslide through a series of experimental tests, a part of which involved wetting tests under anisotropic stress states conducted on unsaturated intact specimens of silty loess. The tests were performed using a manually controlled unsaturated triaxial device (Zhang 2017). The test results showed that the wetting-induced response of the intact loess was a combination of both volumetric and shearing behavior.

The presence of some deficiencies in the reviewed studies (e.g., using manual pressure regulators, using dead weights for axial loading, using a triaxial single cell and plastic connecting pipes) prompted the authors to develop a new fully-automated unsaturated triaxial device that can accurately and continuously follow different hydromechanical stress/strain paths. In order to achieve this goal, two improvements have been considered for the newly developed device which is housed in a temperature and humidity-controlled room. The improvements are as follows:

- A data logger/acquisition system is developed, enabling the continuous measurement of stress/strain variables at a maximum rate of three data per second to capture the sudden deformations of the specimen during long term loadings.
- A user-friendly software is developed using Visual Basic, enabling the definition of the stress/strain variables and the desired stress/strain paths.

To evaluate the performance of the developed apparatus, an experimental program including two stress-controlled wetting tests were conducted to assess the effect of initial shear stress on the hydromechanical behavior of a collapsible loess and exhibit the ability of the developed device.

2. Experimental setup

The developed unsaturated triaxial device consists of a double cell, a load frame, a load cell, a linear variable displacement transducer (LVDT), three pressure transducers, two automated volume change measurement devices, three electro-pneumatic pressure regulators, a data logger/acquisition system, and a controlling software developed and installed on a central computer according to the needs for following any stress, strain and hydromechanical path. The developed fully automated unsaturated triaxial device is shown in Fig. 1.

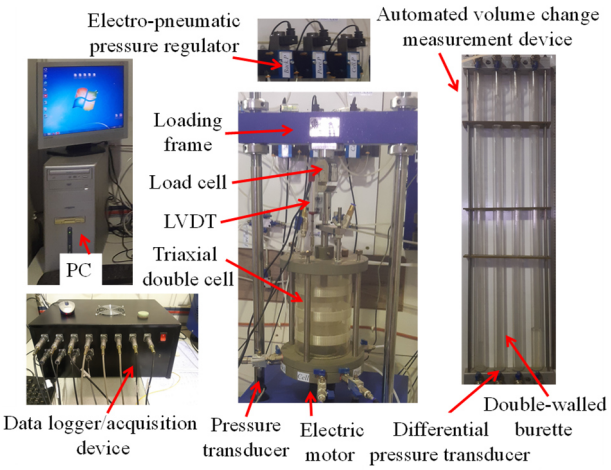

Figure 1. The developed unsaturated triaxial device

The main parts of the apparatus are described in detail as follows:

2.1. Triaxial double cell

As shown in Fig. 2, a new double cell was designed with an integrated structure providing considerable simplicity in assembling and dismantling procedures. The cell top plate, cell bottom plate, base plate, specimen pedestal, and specimen top cap are accurately machined from lightweight anodized aluminum to assure high resistance against corrosion and unacceptable deformation. The double cell body and the base plate are connected through 4 external tie rods, spaced at 90°. The base plate has five valves for inner cell water pressure, inner cell water outlet, pore water pressure, flushing outlet, and air pressure. In addition, there are two valves installed on the outside of the cell bottom plate, for the outer cell water inlet and outlet.

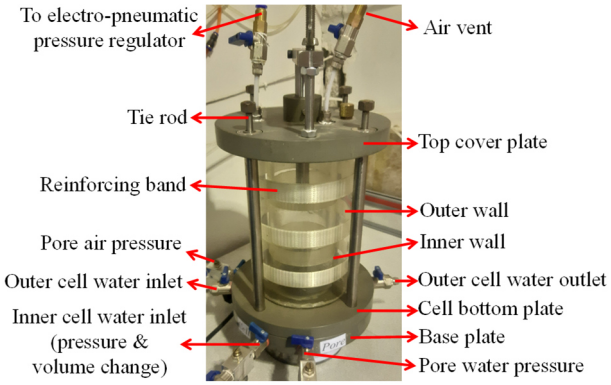

Figure 2. The designed triaxial double cell

The top cover plate has an air vent valve for the inner cell and a valve connected to the electro-pneumatic pressure regulator to provide outer cell water pressure. The inner and outer cell walls are tightly sealed to the top cover and the bottom plates via O-rings to prevent water leakage from the inner cell to the outer cell. Reinforcing fiberglass bands are used around the inner and outer cell walls to increase the stiffness of the double cell. The silicone packing with high sealing performance and negligible friction is used to connect the loading piston and the top cover plate. The specimen pedestal is replaceable and connected to the base plate. A 5-bar high air entry (HAE) ceramic disk with the air entry suction of

500 kPa is embedded in the circular hole of the pedestal and sealed by epoxy resin. In order to flush out the diffused air bubbles, which can be a source of error in the volume change measurement during long-lasting tests, a spiral-grooved water compartment is machined beneath the HAE ceramic disk.

Copper connecting pipes are used to connect different components of the device. The double cell prevents the expansion of the inner cell wall by applying similar pressure on its two sides. However, Ng et al. (2002) reported that despite using the double cell and bronze connecting pipes, there are still small values of both immediate and creep deformations that make it necessary to conduct accurate calibration tests. In this regard, calibration tests were performed using a rigid dummy specimen to calibrate the deformations of the inner cell and connecting pipes over the pressure range of 100 to 700 kPa, as shown in Fig. 3. The calibration results for the copper pipes revealed that no creep deformation occurred over the range of applied pressures.

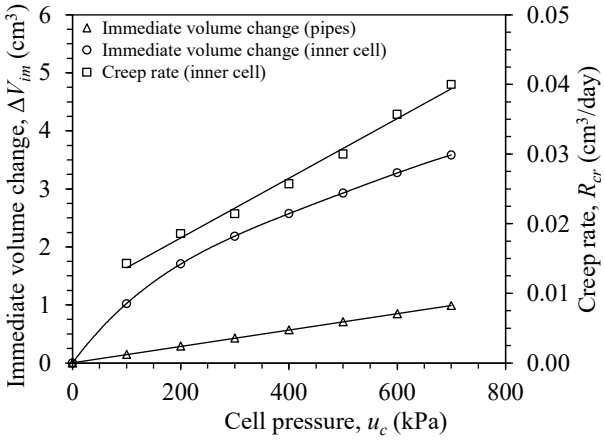

Figure 3. The immediate volume change and creep rate of inner cell and pipes under different applied pressures

2.2. Automated volume change measurement device

The developed volume change measurement device is composed of: (1) double-walled burette, (2) top cover plate, (3) bottom plate, and (4) differential pressure transducer (Fig. 1). In the double-walled burette, the open-ended inner burette is enclosed within the outer burette and sealed at the bottom endplate. The top cover and bottom plates are tightly held together using two external tie rods. The inner burette has an inside diameter and effective height of 0.4 and 100 cm, respectively, resulting in a volume capacity of 12.5 cm^3. In order to avoid water evaporation, a thin layer of light oil is added to the surface of the water in the inner burette. In this setup, the air pressure is applied to the top of both inner and outer burettes simultaneously. Therefore, the same pressure is imposed on both sides of the inner burette wall, eliminating the volume change measurement error caused by pressure-induced expansion. The inner burette is made of glass with no water absorption. The height of the water in the inner burette is continuously monitored by a differential pressure transducer (with an accuracy of 10 Pa; 1 mm of water level), resulting in an accuracy of 0.01 cm^3 for volume change measurement.

2.3. Suction control and measurement

In the unsaturated triaxial device developed in this research, the axis translation technique (Hilf 1956) is used to control the matric suction during unsaturated tests. Before performing each test, the HAE disk should be saturated (Fredlund and Rahardjo 1993). The pore air pressure is applied and measured through a pressure line connected to the top of the low air entry porous stone above the specimen, and pore water pressure is applied and measured through a pressure line connected to the bottom of the HAE disk beneath the specimen. For accurate measurement of the pore water volume change, it is necessary to flush the diffused air bubbles accumulated beneath the HAE disk.

2.4. Axial load/deformation control and measurement

In order to conduct triaxial tests under anisotropic stress states, it is required to control and measure either axial load or axial deformation. The minimum and maximum speed of upward/downward movement of the cell are 2 μm/min and 5 mm/min, respectively. The controlled electric motor can control either the axial load in response to feedback signals from a load cell transducer or the axial deformation in response to feedback signals from an LVDT. As shown in Fig. 1, the load cell transducer (with an accuracy of 1N) is attached to the cross beam of the load frame and the LVDT (with an accuracy of 0.01 mm) is fixed to the loading piston, both located atop the cell.

2.5. Pressure control and measurement (cell pressure, pore water pressure, and pore air pressure)

A high-capacity air compressor is used to supply the cell pressure, pore water pressure, and air pressure required for unsaturated triaxial tests. The air compressor is of screw-type, especially designed for continuous operation during any long unsaturated test. The air compressor has an air tank with a capacity of 0.8 m^3. It can provide an airflow of 1.4 m^3/min with a maximum pressure of 1000 kPa.

A manual air pressure regulator is provided as well, on the input pressure line of the unsaturated triaxial device in order to eliminate pressure fluctuations at each loading/unloading of the screw air compressor. In addition, three software-controlled electro-pneumatic pressure regulators (with an accuracy of 1 kPa) are utilized on the three pressure lines (i.e., cell water, pore air, and pore water) to control the pressures, based on the feedback signals received from three pressure transducers (with an accuracy of 1 kPa).

2.6. Data logger/acquisition system and the controlling software

The control system of the triaxial device comprises an automatic data logger/acquisition device and a controlling software installed on a PC. It is designed to perform any unsaturated triaxial tests along any complex

stress/strain paths under the stress/strain-controlled conditions using the closed-loop feedback technique. All of the measured values are collected by the data logger/acquisition device, converted to the standard units, and saved on the PC at any desired time intervals (maximum rate of three data per second).

2.7. Temperature/humidity-controlled room

The developed unsaturated triaxial device is placed in a temperature/humidity-controlled room constructed from heat-insulating sandwich panels to eliminate the effect of temperature fluctuation of the outside environment on the test results. This room is equipped with an air-conditioning system capable of controlling the temperature and relative humidity with the accuracies of 0.5 °C and 1 %, respectively. The unsaturated tests considered in this study were conducted at the desired temperature of 22 °C. The temperature fluctuation of the temperature-controlled room during the period of two days is presented in Fig. 4.

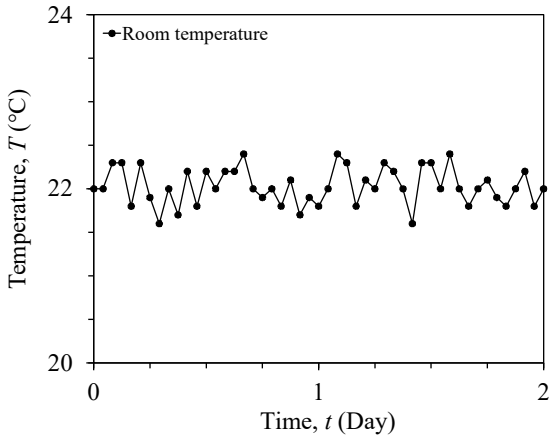

Figure 4. Temperature fluctuation of the temperature-controlled room during the period of two days

3. Materials and specimen preparation

The soil used in this study was taken from Gorgan city in the Golestan province at the North-East of Iran. This region is covered to a large extent by aeolian loessial deposits (Pashaei 1997). A natural soil, collected from a depth of about 1 m, was brought to the laboratory. The average initial water content, w (%), and dry density, γ_d, were 7 % and 14.8 kN/m^3, respectively. The particle size distribution of the soil indicated that the soil contained about 60 % silt, 37 % clay, and 3 % sand. The average plasticity index and liquid limit of the tested soil were 14.7 and 37.9, respectively, with a specific gravity of 2.72. The tested soil is classified as low-plasticity clay (CL) in accordance with ASTM D2488-17e1. Additionally, in accordance with the loess classification proposed by Gibbs and Holland (1960), the examined soil is clayey loess. Based on the results of the filter paper test (ASTM D5298-16) conducted on reconstituted samples prepared with the initial condition similar to the natural soil, the air expulsion value, water entry value, and residual degree of saturation for the examined soil were obtained to be equal to 10 kPa, 1000 kPa, and 0.07, respectively.

The reconstituted soil specimens were prepared by static compaction method using the under-compaction procedure (Ladd 1978). A cylindrical mold, 38 mm in diameter and 76 mm in height, was used for triaxial specimen preparation. To reproduce the hydro-mechanical behavior of the Gorgan clayey loess at natural condition, the initial water content and dry density of the reconstituted specimens were chosen as those of the natural condition. Based on the filter paper test, the initial suction of reconstituted specimens was 900 kPa.

During the specimen preparation procedure, the intact loess cementations, i.e., clay bridges and calcite cementations were mostly destroyed due to grinding and sieving of the soil clods. Accordingly, matric suction should be the primary bonding mechanism that contributes to the structural stability of the reconstituted specimens (Wang et al. 2019a; Mu et al. 2020).

4. Test procedure

The experimental procedure adopted in this research will be described as follows. Hereafter, the terms matric suction, ψ, mean net stress, p_n, deviator stress, q, and net shear stress ratio, η, are defined as:

$$\psi = u_a - u_w \tag{1}$$

$$p_n = \frac{\sigma_1 + 2\sigma_3}{3} - u_a \tag{2}$$

$$q = \sigma_1 - \sigma_3 \tag{3}$$

$$\eta = \frac{q}{p_n} \tag{4}$$

where u_a is pore air pressure, u_w is pore water pressure, σ_1 is major principal total stress, and σ_3 is minor principal total stress.

After saturation of the HAE disk, installing the specimen, and assembling the triaxial cell, both inner and outer cells were filled with de-aired water. Then, the programmed values for the cell pressure, the pore air pressure, the pore water pressure, and the axial load were imposed on the specimen boundary at the desired increment rates introduced to the software (i.e., 1 kPa/sec for cell pressure, air pressure, and water pressure; 1 N/sec for axial load). As the first step, the specimen was subjected to the desired initial shear and mean net stresses, simultaneously by wetting to the target suction of 400 kPa from the initial suction of 900 kPa. Subsequently, after reaching an equilibrium state under the suction of 400 kPa, the specimens were wetted at reduction steps of ψ = 200, 100, 50, 25, 15, 0 kPa by increasing the pore water pressure while keeping the axial load, the cell pressure, and the pore air pressure constant. Two different initial net shear stress ratios (i.e., η_i = 0, 2) under initial mean net stress of p_{ni} = 100 kPa were considered in this study. The initial stress states of the tested specimens (i.e., p_{ni}, q_i, ψ_i, and η_i) are shown in Table 1.

During the tests, the matric suction was lowered to the next step after ensuring that the suction-equilibrium condition was achieved within the soil specimens. The suction-equilibrium condition at the end of each step was assumed to be reached once the rate of change in both

pore water absorption/desorption and specimen volume change became less than 0.14 cm^3/day (Haeri et al. 2014).

Table 1. The initial stress states in the wetting tests

Test	p_{ni} (kPa)	q_i (kPa)	η_i	ψ_i (kPa)
W1	100	0	0	900
W2		200	2	900

It is worthy to note that, despite the application of the constant axial load, the volumetric and axial deformations caused the specimen's cross-sectional area to be continuously changing during the tests, which in turn resulted in variations of deviator stress, q. The stress paths of the wetting tests are plotted in the q - p_n - ψ space in Fig. 5, in which the initial shear stress and mean net stress are assumed to be constant throughout the tests.

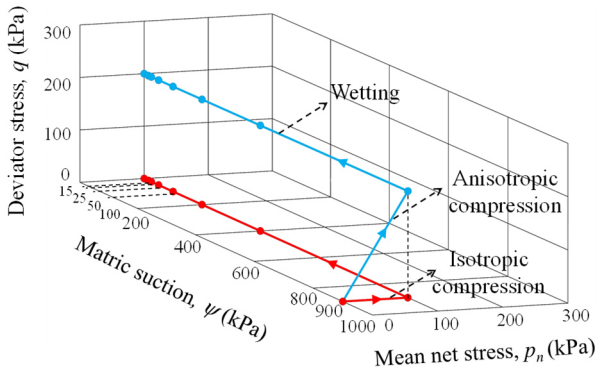

Figure 5. Applied stress paths in two wetting tests

5. Test results

5.1. The functionality of the developed device

In order to evaluate the functionality of the device, the variations of the actual values of pore water pressure, u_w, pore air pressure, u_a, cell pressure, u_c, and axial load, F_v, during two tests are presented in Figs. 6a and 7a. The enlarged portion of these plots are also shown in Fig. 6b (step of ψ = 25 kPa) and Fig. 7b (step of ψ = 100 kPa). It can be seen that the developed apparatus followed the desired stress path accurately, with all the pressures being controlled to ± 1 kPa. In unsaturated tests under an anisotropic stress state, the axial load should be accurately controlled to prevent any undesirable failure of the tested specimens. As can be seen in Fig. 7, the axial load was accurately controlled with ± 4 % deviation from the desired value (i.e., F_v = 0.227 kN) representing the excellent performance of the device. As stated previously, especially in the case of collapsible soils, it is necessary to monitor the deformations of the soil specimen continuously. In this regard, the ability of the device to continuously measure the axial deformation, the specimen volume change, and the pore water volume change during two tests is shown in Fig. 8, which will be described in detail in section 5.2.

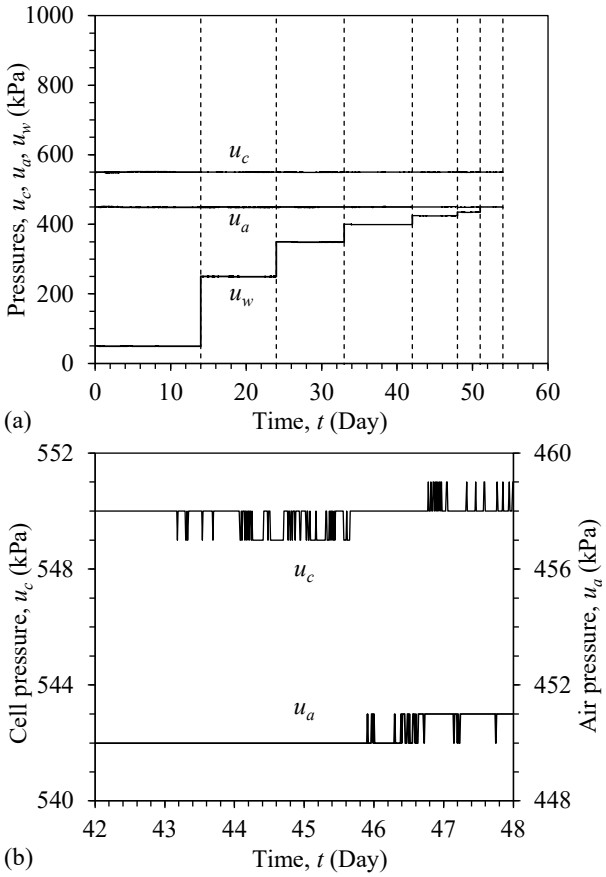

Figure 6. Variations of the u_c, u_a, and u_w in test W1: (a) during full test time period and (b) during the time period of 42 to 48 days under ψ = 25 kPa

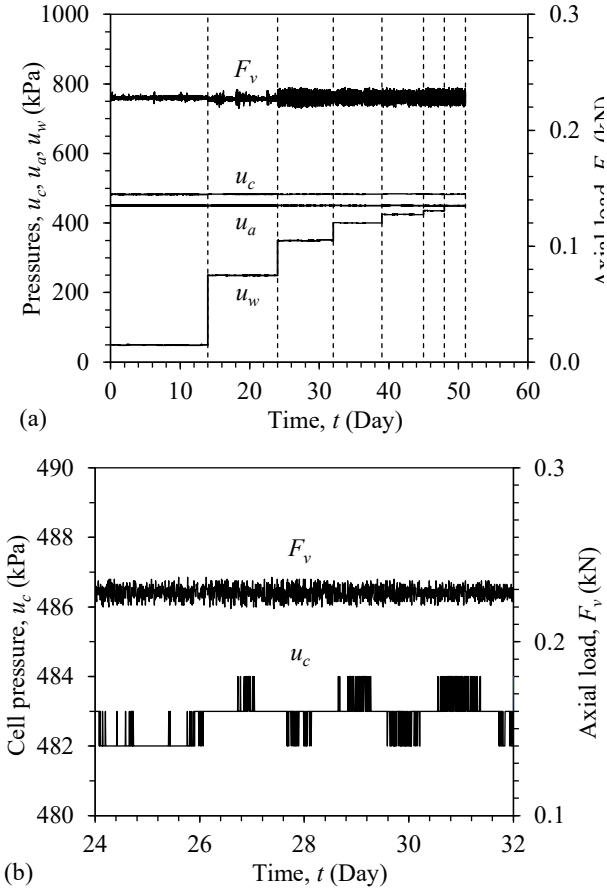

Figure 7. Variations of the u_c, u_a, u_w, and F_v in test W2: (a) during full test time period and (b) during the time period of 24 to 32 days under ψ = 100 kPa

5.2. Wetting tests under isotropic and anisotropic stress paths

The effect of initial shear stress on the hydromechanical behavior of the reconstituted specimens of Gorgan clayey loess was studied through two wetting tests. In addition to one anisotropic test under the effect of initial shear stress (i.e., W2 under $\eta_i = 2$), an isotropic test (i.e., W1 under $\eta_i = 0$) under the same initial mean net stress was also conducted as the reference for highlighting the effect of initial shear stress on the hydromechanical behavior of the examined soil. The obtained results for specimens' volume change, ΔV_v, axial deformation, ΔH, and pore water volume change, ΔV_w, versus elapsed time are presented in Fig. 8. The endpoints of the wetting steps are marked by circle markers. The sign convention adopted here is that the contractive volumetric deformation, contractive axial deformation, and water absorption are positive. Additionally, the positive side of the axes of the volumetric and the axial deformations is assumed to be downward.

As shown in Fig. 8, it is evident that the volume change, the axial deformation, and the water absorption behavior of the tested specimens are considerably affected by the initial shear stress. The specimens showed stepwise compressive deformation regarding the stepwise reduction of imposed matric suction.

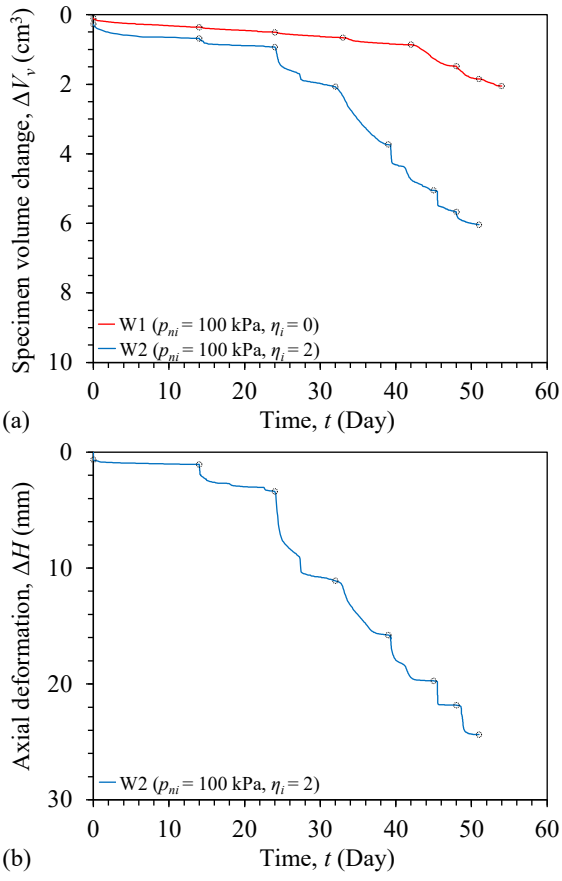

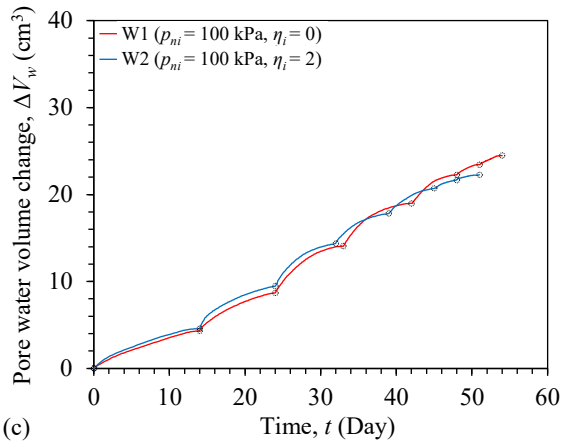

Figure 8. The obtained results from wetting tests versus time: (a) specimen volume change, (b) axial deformation and (c) pore water volume change

By comparing the specimens' volume change, ΔV_v, under isotropic and anisotropic stress states (Fig. 8a), it can be postulated that the application of initial shear stress triggered soil particles to be more prone to slide or disintegrate which resulted in a particle rearrangement with lower porosity. Moreover, as the wetting proceeded, the effect of initial shear stress on the volumetric behavior became more pronounced (e.g., 1.41 cm^3 larger ΔV_v at ψ = 100 kPa; 3.99 cm^3 larger ΔV_v at ψ = 0 kPa for test W2 compared to test W1).

As shown in Fig. 8c, from the early steps of the tests, two specimens started to absorb water as the applied matric suction was reduced in successive steps. A part of this water absorption can be attributed to the water absorbed on the surface of the clay minerals (i.e., illite and chlorite). The other mechanism that contributed to water retention was capillary tension. As the wetting proceeded to suctions close to the saturated condition, by comparing the plots of ΔV_v and ΔV_w for two specimens, it can be deduced that the application of initial shear stress caused the specimen volume to be lowered to such an extent that the water retention capacity of the specimen decreased (e.g., 2.23 cm^3 lower ΔV_w at ψ = 0 kPa for test W2 compared to W1).

Figure 9 presents the variations of volumetric strain, ε_v, axial strain, ε_a, radial strain, ε_r, and shear strain, ε_s, versus matric suction in semi-logarithmic scale during the test W2. The ε_v and ε_a were directly measured during the tests. However, the ε_r and ε_s were calculated based on the measured values of ε_v and ε_a via the equations:

$$\varepsilon_r = \frac{1}{2}(\varepsilon_v - \varepsilon_a) \quad (5)$$

$$\varepsilon_s = \frac{1}{3}(3\varepsilon_a - \varepsilon_v) \quad (6)$$

As shown in Fig. 9, the specimen wetted under the anisotropic stress state (η_i = 2) exhibited an apparent anisotropic straining implying that the wetting-induced collapse of the reconstituted loessial specimen can be considered as a combination of (1) volumetric collapse and (2) shear collapse (Garakani et al. 2015; Wang et al. 2019b).

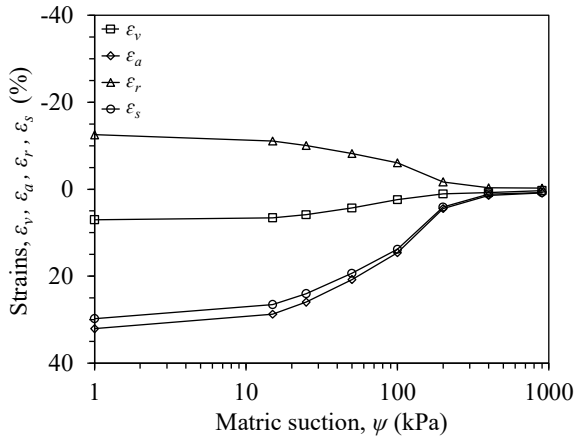

Figure 9. Variations of ε_v, ε_a, ε_r and ε_s during the test W2

The obtained SWRCs data from the wetting tests are presented in Fig. 10. As can be seen, the initial shear stress resulted in a slight increase in the S_r values at a given matric suction as a consequence of an increase in both water absorption and specimen volume reduction (e.g., 5.6 % increase in S_r at ψ = 200 kPa for test W2 compared to test W1).

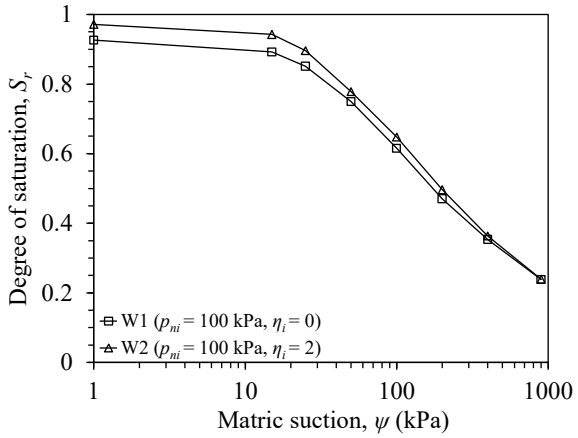

Figure 10. Effect of initial shear stress on the SWRCs

Conclusions

This paper presented an especially developed fully-automated unsaturated triaxial device capable of applying various stress/strain-controlled unsaturated tests with continuously accurate measurement of stress/strain variables. The ability of the developed device for performing tests under anisotropic stress states was evaluated by conducting two wetting tests in order to assess the effect of initial shear stress on the hydromechanical behavior of reconstituted specimens of Gorgan clayey loess.

The results of the experiments showed that the developed apparatus can accurately follow the desired stress path, with all the pressures being controlled to ± 1 kPa. Besides, the axial load can accurately be controlled with ± 4 % deviation from the desired value, representing an excellent performance of the device.

The volumetric behavior of the tested specimens illustrated that at a constant level of initial mean net stress, the specimen wetted under the effect of initial shear stress experienced larger volumetric deformation compared to the specimen wetted under the isotropic stress state. The specimen wetted under anisotropic stress state, exhibited an anisotropic deformation behavior, implying that the wetting-induced collapse of the reconstituted loessial specimen can be considered as a combination of (1) volumetric collapse and (2) shear collapse.

In terms of SWRC, the initial shear stress resulted in a slight increase in the S_r values at a given matric suction as a consequence of an increase in both water absorption and specimen volume reduction.

Acknowledgements

The authors would like to acknowledge the financial support provided by Sharif University of Technology for the development of the testing device to accommodate the required tests for this research. Also, the third author would like to acknowledge the Niroo Research Institute (NRI) for providing with him the opportunity for contribution in this research.

References

Al-Sharrad, M. A. "Evolving anisotropy in unsaturated soils: experimental investigation and constitutive modelling.", Ph.D. Dissertation, University of Glasgow, Scotland, 2013, http://dx.doi.org/10.13140/2.1.2624.6089

Al-Sharrad, M. A., D. Gallipoli, S. J. Wheeler. "Experimental investigation of evolving anisotropy in unsaturated soils.", Géotechnique, 67(12), pp. 1033-1049, 2017, http://dx.doi.org/10.1680/jgeot.15.P.279

ASTM D2488-17e1. "Standard practice for description and identification of soils (visual-manual procedure).", ASTM International, West Conshohocken, PA, USA, 2017, https://doi.org/10.1520/ D2488-17E01

ASTM D5298-16. "Standard test method for measurement of soil potential (suction) using filter paper.", ASTM International, West Conshohocken, PA, USA, 2016, https://doi.org/10.1520/ D5298-16

Borujerdi, S. S. "Development of unsaturated triaxial device in order to conduct stress-controlled tests and study of the hydromechanical behavior of collapsible soils under anisotropic consolidation, a case study of the Gorgan loess.", Master's thesis, Sharif University of Technology, Tehran, Iran, 2015.

Casini, F., V. Serri, S. M. Springman. "Hydromechanical behavior of a silty sand from a steep slope triggered by artificial rainfall: from unsaturated to saturated conditions.", Can Geotech J, 50(1), pp. 28-40, 2013, https://doi.org/10.1139/cgj-2012-0095

Fredlund, D. G., H. Rahardjo. "Soil mechanics for unsaturated soils.", John Wiley & Sons, New York, USA, 1993.

Garakani, A. A., S. M. Haeri, A. Khosravi, G. Habibagahi. "Hydro-mechanical behavior of undisturbed collapsible loessial soils under different stress state conditions.", Eng Geol, 195, pp. 28-41, 2015, http://dx.doi.org/10.1016/j.enggeo.2015.05.026

Gibbs, H. J., W. Y. Holland. "Petrographic and engineering properties of loess.", Technical Information Branch, Denver Federal Center, 28, pp. 1-37, 1960, https://doi.org/10.2136/sssaj1961.03615995002500050007x

Haeri, S. M. "Hydro-mechanical behavior of collapsible soils in unsaturated soil mechanics context.", Japanese Geotechnical Society Special Publication, 2(1), pp. 25-40, 2016, http://dx.doi.org/10.3208/jgssp.KL-3

Haeri, S. M., A. A. Garakani, A. Khosravi, and C. L. Meehan. "Assessing the hydro-mechanical behavior of collapsible

soils using a modified triaxial test device.", ASTM Geotech Test J, 37(2), pp. 190-204, 2014, http://dx.doi.org/10.1520/GTJ20130034

Haeri, S. M., A. Khosravi, A. A. Garakani, S. Ghazizadeh. "Effect of soil structure and disturbance on hydromechanical behavior of collapsible loessial soils.", ASCE Int J Geomech, 17(1), pp. 04016021, 2017, http://dx.doi.org/10.1061/(ASCE)GM.1943-5622.0000656

Haeri, S. M., A. Zamani, A. A. Garakani. "Collapse potential and permeability of undisturbed and remolded loessial soil samples.", In Unsaturated soils: Research and applications, Springer, Berlin, Heidelberg, 2012, pp. 301-308, http://dx.doi.org/10.1007/978-3-642-31116-1_41

Hilf, J. W. "An investigation of pore-water pressure in compacted cohesive soils.", Ph.D. Dissertation, University of Colorado at Boulder, Boulder, CO, USA, 1956.

Hossen, S. B. "Stress dependent water retention curve and volumetric behaviour of intact and re-compacted loess.", Ph.D. Dissertation, The Hong Kong University of Science and Technology, Hong Kong, 2015, http://dx.doi.org/10.14711/thesis-b1552120

Jotisankasa, A., A. Ridley, M. Coop. "Collapse behavior of compacted silty clay in suction-monitored oedometer apparatus.", ASCE J Geotech Geoenviron, 133(7), pp. 867-877, 2007, http://dx.doi.org/10.1061/(ASCE)1090-0241(2007)133:7(867)

Kato, S., K. Kawai. "Deformation characteristics of a compacted clay in collapse under isotropic and triaxial stress state.", Soils Found, 40(5), pp. 75-90, 2000, http://dx.doi.org/10.3208/sandf.40.5_75

Ladd, R. S. "Preparing test specimens using undercompaction.", ASTM Geotech Test J, 1(1), pp. 16-23, 1978, http://dx.doi.org/10.1520/GTJ10364J

Li, P., S. K. Vanapalli, T. Li. "Review of collapse triggering mechanism of collapsible soils due to wetting.", J Rock Mech Geotech Eng, 8(2), pp. 256-274, 2016, http://dx.doi.org/10.1016/j.jrmge.2015.12.002

Liang, C., C. Cao, S. Wu. "Hydraulic-mechanical properties of loess and its behavior when subjected to infiltration-induced wetting.", Bull Eng Geol Environ, 77(1), pp. 385-397, 2018, http://dx.doi.org/10.1007/s10064-016-0943-x

Mu, Q. Y., C. Zhou, C. W. W. Ng. "Compression and wetting induced volumetric behavior of loess: macro-and micro-investigations.", Transp Geotech, 23, pp.100345, 2020, http://dx.doi.org/10.1016/j.trgeo.2020.100345

Ng, C. W. W., L. T. Zhan, Y. J. Cui. "A new simple system for measuring volume changes in unsaturated soils.", Can Geotech J, 39(3), pp. 757-764, 2002, http://dx.doi.org/10.1139/t02-015

Pashaei, A. "Study of physical and chemical characteristics and the source of loess deposits in Gorgan and plain region.", Earth science journal, Iranian geology organization, 23, pp. 67-78, 1997.

Pereira, J. H., D. G. Fredlund. "Volume change behavior of collapsible compacted gneiss soil.", ASCE J Geotech Geoenviron, 126(10), pp. 907-916, 2000, http://dx.doi.org/10.1061/(ASCE)1090-0241(2000)126:10(907)

Sun, D. A., H. Matsuoka, Y. F. Xu. "Collapse behavior of compacted clays in suction-controlled triaxial tests.", ASTM Geotech Test J, 27(4), pp. 362-370, 2004, http://dx.doi.org/10.1520/GTJ11418

Wang, J. D., P. Li, Y. Ma, S. K. Vanapalli. "Evolution of pore-size distribution of intact loess and remolded loess due to consolidation.", J Soils Sediments, 19(3), pp. 1226-1238, 2019a, http://dx.doi.org/10.1007/s11368-018-2136-7

Wang, J., D. Zhang, N. Wang, T. Gu. "Mechanisms of wetting-induced loess slope failures.", Landslides, 16(5), pp. 937-953, 2019b, http://dx.doi.org/10.1007/s10346-019-01144-4

Zhan, L. "Field and laboratory study of an unsaturated expansive soil associated with rain-induced slope instability.", Ph.D. Dissertation, Hong Kong University of Science and Technology, Hong Kong, 2003, http://dx.doi.org/10.14711/thesis-b805488

Zhan, T. L. T., R. Chen, C. W. W. Ng. "Wetting-induced softening behavior of an unsaturated expansive clay.", Landslides, 11(6), pp. 1051-1061, 2014, http://dx.doi.org/10.1007/s10346-013-0449-6

Zhang, D. F. "Behaviours of hydro-mechanical and laws of water and gas permeability during wetting for intact loess.", Ph.D. Dissertation, Xi'an University of Technology, Xi'an, China, 2017.

Zhang, D., J. Wang, C. Chen, S. Wang. "The compression and collapse behavior of intact loess in suction-monitored triaxial apparatus.", Acta Geotech, 15(2), pp. 529-548, 2020, https://doi.org/10.1007/s11440-019-00829-3

Zhou, Y. "Study on landslides in loess slope due to infiltration.", Ph.D. Dissertation, University of Hong Kong, Hong Kong, 2012, http://dx.doi.org/10.5353/th_b4819939

Zhou, Y. F., L. G. Tham, W. M. Yan, F. C. Dai, L. Xu. "Laboratory study on soil behavior in loess slope subjected to infiltration.", Eng Geol, 183, pp. 31-38, 2014, http://dx.doi.org/10.1016/j.enggeo.2014.09.010